JOURNAL OF THERMOPHYSICS AND HEAT TRANSFER
Vol. 24, No. 3, July–September 2010

Technical Notes

Suitability of Multispectral Radiation Thermometry Emissivity Models for Predicting Steel Surface Temperature

Chang-Da Wen* and Chien-Tsai Lu
National Cheng Kung University
Tainan 701, Taiwan, Republic of China

DOI: 10.2514/1.47810

Nomenclature

a_0, a_1	=	unknown coefficients in the emissivity model
c_1	=	first thermal radiation constant
c_2	=	second thermal radiation constant
$L_{\lambda,b}$	=	spectral intensity of blackbody radiation
$L_{\lambda,\mathrm{gen}}$	=	generated spectral intensity of radiation
$L_{\lambda,\mathrm{meas}}$	=	measured spectral radiation intensity
m	=	number of unknown coefficients of emissivity model
N	=	total number of wavelengths available in the examined wavelength range
n	=	required minimum number of wavelengths
T	=	surface temperature
T_λ	=	spectral radiance temperature (equivalent blackbody temperature of the measured spectral intensity)
ε_λ	=	spectral emissivity
λ	=	wavelength
χ^2	=	least-squares error

Subscripts

b	=	blackbody
gen	=	generated
meas	=	measured
λ	=	spectral

I. Introduction

MANY processes in steel manufacturing, such as extruding and rolling, are required to accurately measure the surface temperature in order to attain desired mechanical properties, ensure product quality and reproducibility, and reduce cost. The thermocouple and other types of contact thermometers are very commonly used to measure the surface temperature in industry. However, in some processes, methods of contact temperature measurement are undesirable because the physical contact may not be feasible in moving-material situations and may change the surface physically or chemically. Therefore, accurate noncontact radiation thermometry is highly desired for steel production.

Determining the temperature can be accomplished by three categories of radiation thermometry that use radiance measurement at different number of wavelengths: spectral, dual-wavelength, and multispectral. Spectral radiation thermometry requires the radiance measurement at one wavelength and a constant emissivity value to infer the surface temperature. Dual-wavelength radiation thermometry (DWRT) uses the radiance measurements at two distinct wavelengths and an emissivity compensation algorithm to obtain the surface temperature. Multispectral radiation thermometry (MRT) employs the radiance measurements at three or more discrete wavelengths and an emissivity model to determine the surface temperature. Because of the complex nature of emissivity behaviors of steel, the spectral and dual-wavelength radiation thermometry methods have limited use in specific applications and well-defined situations. The present study is based on the MRT method.

Test samples encompassing a variety of steel were divided into three groups: stainless steel (AISI 420 and AISI 630), hot-work tool steel (AISI H10 and AISI H13), and cold-work tool steel (AISI A2 and AISI A6). Spectral intensity values were first measured for steel alloys over the wavelength range of 2.91 to 4.13 μm and temperatures of 700, 800, and 900 K. The experimental work was then complemented by six MRT emissivity models encompassing mathematical and analytical functions to explore the accuracy of these models at inferring surface temperature subject to the interdependent parametric effects of the number of wavelengths, alloy composition, temperature, and emissivity values.

II. Experimental Methods

The experimental apparatus were mainly composed of a spectrometer (radiation thermometer), test sample heating assembly, temperature controller, power supply, translation stage, data acquisition system, and a blackbody for calibration.

A fast infrared array spectrometer (model ES100, Spectraline, Inc.) was optically aligned in front of the test module. It was used to simultaneously measure 160 discrete spectral radiation intensity values from the examined wavelength range. The radiation intensity from the target is incident on the entrance slit and then ultimately dispersed over a staggered 160-element linear array PbSe detector. The voltages and pixel numbers provided by the linear array are converted into wavelengths and intensities using preinstalled calibration curves. The intensity data collected in each spectrum are stored at 390 Hz. In addition, an alignment HeNe laser can be installed to point the spectrometer at a desired target that is far away from the spectrometer. The data acquisition is controlled by the drive circuit on the spectrometer. A Windows-based graphical user interface (GUI) (Infraspec version 2, Spectraline, Inc.) is available for basic spectrometric functions. The output can either be displayed on the Windows-based GUI or stored onto the computer memory for data analysis.

The sample heating assembly (which includes cartridge heaters, heating block, test sample, and ceramic fiber blanket insulation) is shown in Fig. 1. The whole sample heating assembly was fastened by the aluminum frame and situated on a two-dimensional translation stage. The steel test sample was held in contact with a heating block. To minimize the temperature gradient, the heating block was fabricated from brass and surrounded by a thick blanket of high-temperature ceramic fiber insulation. Three embedded cartridge heaters as the heat source were embedded in the heating block, and a temperature controller with a type-K thermocouple attached on the sample surface was used to heat the sample to the desired test temperature.

As shown in Table 1, six different kinds of steel samples encompassing a broad range of application are divided into three groups and used to evaluate the MRT emissivity models for predicting the surface temperature; they are stainless steel (AISI 420

Received 25 October 2009; revision received 9 February 2010; accepted for publication 20 February 2010.

*Department of Mechanical Engineering, No. 1 University Road; alexwen@mail.ncku.edu.tw (Corresponding Author).

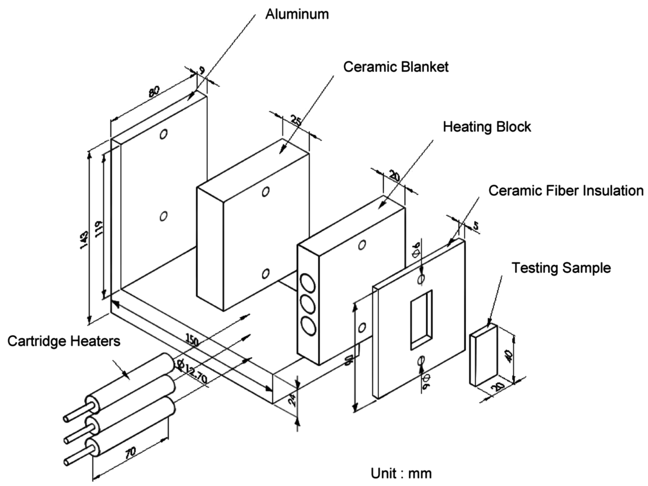

Fig. 1 Construction of steel test sample and heating assembly.

and AISI 630), hot-work tool steel (AISI H10 and AISI H13), and cold-work tool steel (AISI A2 and AISI A6).

After the samples were machined to size, the test surface was cleaned in succession with acetone and methanol to get rid of the oils, grease, or dirt. The tested samples were handled with great care and wrapped in fine tissue to ensure that their surfaces were free from contact with roughening agents.

The heating block was preheated to a temperature slightly above the anticipated one before heating the test sample. The test sample was then pressed against the preheated heating block to initiate heating. The desired temperature was achieved by using the temperature controller to manipulate power input to the cartridge heaters. Once the temperature of the sample was stabilized, the intensity data were ready to be collected.

III. Multispectral Radiation Thermometry

Two different mathematical techniques of multispectral radiation thermometry are used to infer the temperature. The first method is the exact technique that employs an emissivity model with m unknown coefficients and radiation intensity measurements at $m+1$ wavelengths to infer temperature. Coates [1] and Doloresco [2] concluded that the exact technique might cause overfitting and result in large errors when using more than three wavelengths. The other method that can overcome the overfitting problem is the least-squares technique. It employs least-squares fitting of the measured intensities to simultaneously deduce the best-fit values of emissivity and temperature. The least-squares technique requires spectral intensity measurements at a minimum of $m+2$ wavelengths to use an emissivity model with m unknown coefficients. This technique is commonly used in MRT.

The rationale is to determine the inferred temperature and the unknown emissivity coefficients by minimizing the chi-squared (χ^2) value of the following equation:

$$\chi^2 = \sum_{i=0}^{n} (L_{\lambda,\mathrm{meas},i} - L_{\lambda,\mathrm{gen},i})^2 \tag{1}$$

where $L_{\lambda,\mathrm{meas},i}$ and $L_{\lambda,\mathrm{gen},i}$ are the measured and generated values of spectral intensity, respectively. Neglecting the intensity of irradiation from the surroundings that is reflected by the target surface and applying Planck blackbody distribution, the generated spectral intensity can be simplified as

$$L_{\lambda,\mathrm{gen}}(\lambda, T) \cong \varepsilon_\lambda(\lambda)\, L_{\lambda,b}(\lambda, T) = \varepsilon_\lambda(\lambda)\, \frac{c_1}{\lambda^5\,(e^{c_2/\lambda T} - 1)} \tag{2}$$

where $c_1 = 1.191062 \times 10^8\ \mathrm{W} \cdot \mu\mathrm{m}^4 \cdot \mathrm{m}^{-2} \cdot \mathrm{sr}^{-1}$ and $c_2 = 1.438786 \times 10^4\ \mu\mathrm{m} \cdot \mathrm{K}$.

For emissivity models with exponential form, the linear least-squares technique can be used to determine the inferred temperature and the unknown emissivity coefficients by minimizing the magnitude of χ^2 in the following equation:

$$\chi^2 = \sum_{i=0}^{n} (\ln L_{\lambda,\mathrm{meas},i} - \ln L_{\lambda,\mathrm{gen},i})^2 \tag{3}$$

In addition, the Planck blackbody distribution used in Eq. (2) to determine the generated value of spectral intensity $L_{\lambda,\mathrm{gen},i}$ is approximated by Wien's formula:

$$L_{\lambda,b}\,(\lambda, T) = \frac{c_1}{\lambda^5\,(e^{c_2/\lambda T} - 1)} \cong \frac{c_1}{\lambda^5\,(e^{c_2/\lambda T})} \tag{4}$$

Therefore, a set of equations that is linear with respect to the temperature and the unknown emissivity coefficients can be created to simplify the computation.

The unfixed coefficient values in the emissivity model allow the multispectral radiation methods to have enough selectivity to represent the variable emissivity behaviors and are less affected by noise. Moreover, the increased number of wavelengths also allow for the statistical reduction in temperature errors from measurement noise.

As shown in Table 2, six selected MRT emissivity models encompassing mathematical and analytical functions are examined in this study for accuracy in temperature determination: the Hagen–Rubens relation (HRR) model [3–9], inverse spectral temperature (IST) model [6–9], inverse wavelength squared (IWS) model [7–10], wavelength temperature (WLT) model [6,8,9,11], and two variations to IST and WLT models (IST* and WLT*).

IV. Results and Discussion

Table 3 provides absolute errors in the inferred temperature predicted by six MRT emissivity models, HRR, IST, IST*, IWS, WLT, and WLT*. Values exceeding ±50 K have been purposely deleted to help point out accurate models and their predictive trends. The results are shown for three groups of steel samples: stainless steel (AISI 420 and AISI 630), hot-work tool steel (AISI H10 and AISI H13), and cold-work tool steel (AISI A2 and AISI A6); two different number of wavelengths (n and N); and three different temperatures (700, 800, and 900 K). The value n is the required minimum number of wavelengths using the least-squares technique, which is equal to the number of unknown coefficients in the emissivity model plus two, and N is the total number of wavelengths available in the examined wavelength range. A comprehensive analysis of these results yields some useful conclusions and trends. Below is a discussion of the effects of the number of wavelengths, alloy

Table 1 Steel alloys tested in present study

Type		Applications
Stainless steel	AISI 420	Bolt, palletizer, scalpel, die (plastic)
	AISI 630	Shaft, bolt, valve, family appliance, scalpel, food Machine, die (plastic)
Hot-work tool steel	AISI H10	Shaft, bolt, die (casting, forging, extrusion),
	AISI H13	Pin, die (casting, extrusion, plastic)
Cold-work tool steel	AISI A2	Shaft, accuracy gauge, die (casting, trimming, roller)
	AISI A6	Punch, roller, accuracy gauge, die (casting, trimming)

Table 2 Mathematical form of emissivity models examined in present study

Emissivity model	Mathematical function	n
Hagen–Rubens relation	$\varepsilon_\lambda = a_0 \times (\frac{T}{\lambda})^{1/2}$	3
Inverse spectral temperature-1	$\varepsilon_\lambda = \exp(\frac{a_0}{T_\lambda})$	3
Inverse spectral temperature-2	$\varepsilon_\lambda = \exp(a_0 + \frac{a_1}{T_\lambda})$	4
Inverse wavelength squared	$\varepsilon_\lambda = \frac{1}{1+a_0\lambda^2}$	3
Wavelength temperature-1	$\varepsilon_\lambda = \exp(a_0\lambda + a_1 T)$	4
Wavelength temperature-2	$\varepsilon_\lambda = \exp(a_0\lambda + \frac{a_1}{T_\lambda})$	4

composition, temperature, and emissivity values as they relate to temperature prediction for the MRT emissivity models.

A first look at the table appears to be somewhat puzzling. However, more than one-half of the results provide the absolute temperature error under ± 50 K and more than one-fourth of them are under ± 15 K. The occurrence of accurate measurements that have errors below 5 K is random. They are the HRR model for AISI A2 and AISI A6 at 900 K; the IST* model for AISI H10 at 800 K; the IWS model for AISI 420 and AISI H10 at 700 K, and AISI H13 and AISI A2 at 800 K; the WLT model for AISI 420, AISI A2, and AISIA6 at 800 K; and the WLT* model for AISI 630 at 800 and 900 K. Statistically, two emissivity models, WLT and IWS, give good results most frequently and provide the best overall compensation for different alloys, number of wavelengths, and temperatures. Overall, the IST model shows the poorest compensation and is not recommended for a steel sample in MRT.

One feature that makes MRT more preferred than spectral radiation thermometry (SRT) and DWRT is that an increase in the number of wavelengths allows for the statistical reduction in temperature errors from measurement noise. However, as the results show in Table 3, increasing the number of wavelengths does not really enhance measurement accuracy for most models. The required minimum number of wavelengths n actually gives satisfactory results using either linear or nonlinear least-squares technique in this study. Similar results have also been reported by Doloresco [2], Gathers [12], and Gardner et al. [13]. Therefore, it is sufficient to employ the required minimum number of wavelengths to infer the temperature.

Table 4 shows the comparison between the SRT method and the MRT method. According to the experimental measurements, at wavelength $\lambda = 3.51\ \mu$m the constant emissivity values chosen in SRT are 0.5 at 700 K, 0.7 at 800 K, and 0.9 at 900 K. The WLT model at 700 and 800 K and the IWS model at 900 K are chosen for the examination of the MRT method. The results show that the MRT method with the required minimum number of wavelengths achieves much better temperature prediction than the SRT method. Therefore,

Table 3 Absolute temperature errors in Kelvin, from 2.91–4.13 μm in inferred temperature by MRT, for steel samples at 700, 800, and 900 K[a]

	HRR		IST		IST*		IWS		WLT		WLT*	
Sample T, K	n	N	n	N	n	N	n	N	n	N	n	N
Stainless steel AISI 420												
700	——	——	——	——	——	——	−4.2	−21.2	−27.1	−16.2	41.1	——
800	——	——	——	——	−9.1	——	−16.2	−18.6	8.7	1.1	——	——
900	——	——	——	——	——	——	−9.9	−7.8	12.6	17.1	——	——
Stainless steel AISI 630												
700	35.4	36.0	34.0	32.6	——	−8.2	——	——	−29.9	−36.5	40.1	31.5
800	——	45.3	28.9	17.0	−17.7	——	——	——	——	——	4.7	13.5
900	——	43.3	14.9	8.3	——	——	——	——	——	——	1.5	6.4
Hot-work tool steel AISI H10												
700	−9.6	−11.0	40.0	42.3	9.0	8.0	12.6	0.9	15.4	18.0	38.1	42.5
800	−11.8	7.2	——	——	2.9	3.0	−35.1	31.7	37.1	39.1	——	——
900	——	——	——	——	——	——	6.8	−8.4	35.4	19.1	——	——
Hot-work tool steel AISI H13												
700	——	48.8	35.7	16.2	——	——	−30.7	——	——	——	−8.3	7.4
800	——	——	——	——	——	——	5.8	4.1	21.5	25.2	——	——
900	——	——	——	——	——	6.4	30.3	25.6	——	——	——	——
Cold-work tool steel AISI A2												
700	——	——	——	——	——	−31.8	22.2	20.3	20.2	35.2	——	——
800	−6.9	−27.2	——	36.6	−21.4	−27.7	11.8	3.6	3.6	4.5	31.1	30.9
900	−1.5	−2.3	——	——	−25.0	−25.0	7.2	12.8	23.4	29.6	——	——
Cold-work tool steel AISI A6												
700	37.0	13.3	44.9	——	−22.2	−22.3	−25.1	39.2	8.1	21.9	26.6	42.5
800	——	——	9.7	12.0	−14.9	−14.6	−6.9	−6.8	−2.1	−2.0	13.4	12.2
900	−2.2	3.9	——	——	——	−74.2	10.2	10.7	35.6	31.9	——	——

[a]Missing values correspond to errors beyond ± 50 K.

Table 4 Comparison of the percentage of temperature error between SRT and MRT methods

Model T	AISI 420	AISI 630	AISI H10	AISI H13	AISI A2	AISI A6
700 K						
SRT ($\varepsilon = 0.5$)	10.6	11.9	11.6	16.9	2.3	10.5
WLT	0.7	4.3	2.2	10.2	2.9	1.2
800 K						
SRT ($\varepsilon = 0.7$)	10.3	20.3	6.7	10.7	3.2	4.5
WLT	7.9	9.0	1.6	2.7	0.5	0.3
900 K						
SRT ($\varepsilon = 0.9$)	12.6	24.9	11.1	12.2	6.9	2.4
IWS	1.1	10.7	0.8	3.4	0.8	1.1

Table 5 Percentage of temperature error in inferred temperature by MRT for steel samples[a]

Sample, T	HRR	IST	IST*	IWS	WLT	WLT*
		$\varepsilon \leqq 0.3$				
AISI 420, 700 K	——	——	——	0.6	3.9	——
AISI H13, 700 K	——	——	——	4.4	——	1.2
AISI 630, 700 K	——	4.9	——	——	4.3	——
AISI 630, 800 K	——	3.6	2.2	——	——	0.6
AISI 630, 900 K	——	1.7	——	——	——	0.2
		$0.3 < \varepsilon < 0.6$				
AISI A2, 700 K	——	——	——	3.2	2.9	——
AISI 420, 800 K	——	——	1.1	2.0	1.1	——
AISI 420, 900 K	——	——	——	1.1	1.4	——
AISI H13, 800 K	——	——	——	0.7	2.7	——
AISI H13, 900 K	——	——	——	3.4	——	——
AISI H10, 900 K	——	——	——	0.8	3.9	——
		$\varepsilon \geqq 0.6$				
AISI H10, 700 K	1.4	——	1.3	1.8	2.2	——
AISI H10, 800 K	——	2.0	1.4	0.2	1.6	2.2
AISI A2, 800 K	0.9	——	2.7	1.5	0.5	3.9
AISI A2, 900 K	0.2	——	2.8	0.8	2.6	——
AISI A6, 700 K	——	——	3.2	3.6	1.2	3.8
AISI A6, 800 K	——	1.2	1.9	0.9	0.3	1.7
AISI A6, 900 K	0.2	——	——	1.1	4.0	——

[a]Missing values correspond to errors beyond 5%.

without known emissivity information, the MRT method is preferred for its ability to enhance measurement accuracy as well as to account for the complex emissivity behaviors.

Table 5 shows the effects of emissivity values on MRT temperature prediction. The percentages of inferred temperature error predicted by MRT are given for six models using the required minimum number of wavelengths in the spectral range from 2.91 to 4.13 μm. To help point out any useful trends, only values below 5% are shown in the table. According to the experimental data of spectral emissivity for all test alloys, the emissivity values can be generally divided into three regions: smaller than 0.3, between 0.3 and 0.6, and higher than 0.6. From the results, the better performance is apparently found in the large-emissivity-value region. When the emissivity value is between 0.3 and 0.6, only the IWS and WLT models perform well. When the emissivity value is below 0.3, the good results are found less and randomly. Therefore, a higher emissivity value shows better MRT temperature prediction. For most metallic surfaces, the emissivity typically increases with increasing temperature. This leads to the inference that for a steel surface, more accurate temperature measurement by MRT can be achieved at higher temperatures.

V. Conclusions

Experiments were performed to measure the spectral intensity values of a variety of steel samples at 700, 800, and 900 K. The experimental work is coupled with six selected emissivity models encompassing mathematical and analytical functions to examine MRT for inferring surface temperature. Assessment of MRT emissivity models is subject to parametric effects, such as number of wavelengths, alloy composition, temperature, and emissivity values. The data show that more than one-half of the temperature predictions by MRT emissivity models provide the absolute temperature error under $\pm$50 K, and more than one-quarter of the results are under $\pm$15 K. Increasing the number of examined wavelengths in MRT does not significantly improve temperature prediction. However, the MRT method with the required minimum number of wavelengths still performs better than the SRT (spectral radiation thermometry) method. More accurate temperature measurement by MRT can be achieved at higher temperatures. Overall, two emissivity models, WLT and IWS, provide the best compensation for the aforementioned parametric influences.

Acknowledgments

The authors are grateful for the support of the National Science Council of Taiwan (with project number NSC-94-2218-E-006-046). The authors would also like to thank the Gloria Material Technology Corporation (GMTC) in Taiwan for the supply of steel samples and Jongmook Lim of Spectraline, Inc., for the technical assistance and the instrument support.

References

[1] Coates, P. B., "Multi-Wavelength Pyrometry," *Metrologia*, Vol. 17, No. 3, 1981, pp. 103–109. doi:10.1088/0026-1394/17/3/006

[2] Doloresco, B. K., "Review of Multispectral Radiation Thermometry and Development of Constrained Minimization Method," M.S. Thesis, Purdue Univ., West Lafayette, IN, 1986.

[3] Dmitriev, V. D., and Kholopov, G. K., "Radiant Emissivity of Tungsten in the Infrared Region of the Spectrum," *Zhurnal Prikladnoi Spektroskopii*, Vol. 2, No. 6, 1965, pp. 481–488.

[4] Haugh, M. J., "Radiation Thermometry in the Aluminum Industry," *Theory and Practice of Radiation Thermometry*, edited by D. P. DeWitt, and G. D. Nutter, Wiley, New York, 1988, pp. 905–971.

[5] Mihalow, F. A., "Radiation Thermometry in the Steel Industry," *Theory and Practice of Radiation Thermometry*, edited by D. P. DeWitt, and G. D. Nutter, Wiley, New York, 1988, pp. 861–904.

[6] Pellerin, M. A., "Multispectral Radiation Thermometry: Emissivity Compensation Algorithm," M.S. Thesis, Purdue Univ., West Lafayette, IN, 1990.

[7] Pellerin, M. A., "Multispectral Radiation Thermometry for Industrial Application," Ph.D. Thesis, Purdue Univ., West Lafayette, IN, 1999.

[8] Wen, C., and Mudawar, I., "Emissivity Characteristics of Roughened Aluminum Alloy Surfaces and Assessment of Multispectral Radiation Thermometry (MRT) Emissivity Models," *International Journal of Heat and Mass Transfer*, Vol. 47, 2004, pp. 3591–3605. doi:10.1016/j.ijheatmasstransfer.2004.04.025

[9] Wen, C., "Emissivity characteristics of Aluminum Alloy Surfaces and Assessment of Multispectral Radiation Thermometry (MRT) Emissivity Models," Ph.D. Thesis, Purdue Univ., West Lafayette, IN, 2005.

[10] Duvaut, T., Georgeault, D., and Beaudoin, J. L., "Multiwavelength Infrared Pyrometer: Optimization and Computer Simulations," *Infrared Physics and Technology*, Vol. 36, No. 7, 1995, pp. 1089–1103. doi:10.1016/1350-4495(95)00040-2

[11] Dail, G. J., Fuhrman, M. G., and DeWitt, D. P., "Evaluation and Extension of the Spectral-Ratio Radiation Thermometry Method," *Proceedings 4th International Aluminum Extrusion Technology Seminar*, Vol. 2, Chicago, 1988, pp. 209–213.

[12] Gathers, G. R., "Analysis of Multiwavelength Pyrometry Using Nonlinear Chi-square Fits and Monte Carlo Methods," *International Journal of Thermophysics*, Vol. 13, No. 3, 1992, pp. 539–554. doi:10.1007/BF00503888

[13] Gardner, J .L., Jones, T. P., and Davies, M. R., "A Six-Wavelength Radiation Pyrometer," *High Temperatures—High Pressures*, Vol. 13, 1981, pp. 459–466.